DEVELOPMENT AND TEST OF A DIGITALLY STEERED ANTENNA ARRAY FOR THE NAVIGATOR GPS RECEIVER

Heitor David Pinto, Jennifer E. Valdez, Luke M. B. Winternitz
Munther A. Hassouneh, Samuel R. Price
Components and Hardware Systems Branch
NASA Goddard Space Flight Center

ABSTRACT

Global Positioning System (GPS)-based navigation has become common for low-Earth orbit spacecraft as the signal environment is similar to that on the Earth's surface. The situation changes abruptly, however, for spacecraft whose orbital altitudes exceed that of the GPS constellation. Visibility is dramatically reduced and signals that are present may be very weak and more susceptible to interference. GPS receivers effective at these altitudes require increased sensitivity, which often requires a high-gain antenna. Pointing such an antenna can pose a challenge. One efficient approach to mitigate these problems is the use of a digitally steered antenna array. Such an antenna can optimally allocate gain toward desired signal sources and away from interferers.

This paper presents preliminary results in the development and test of a digitally steered antenna array for the Navigator GPS research program at NASA's Goddard Space Flight Center. In particular, this paper highlights the development of an array and front-end electronics, the development and test of a real-time software GPS receiver, and implementation of three beamforming methods for combining the signals from the array. Additionally, this paper discusses the development of a GPS signal simulator which produces digital samples of the GPS L1C/A signals as they would be received by an arbitrary antenna array configuration. The simulator models transmitter and receiver dynamics, near-far and multipath interference, and has been a critical component in both the development and test of the GPS receiver.

The GPS receiver system was tested with real and simulated GPS signals. Preliminary results show that performance improvement was achieved in both the weak signal and interference environments, matching analytical predictions. This paper summarizes our initial findings and discusses the advantages and limitations of the antenna array and the various beamforming methods.

INTRODUCTION

The Global Positioning System (GPS) was designed for users on or near the surface of the Earth, and the GPS satellites correspondingly direct their transmissions toward the Earth. Space-based GPS receivers must deal with the high dynamics of orbital motion and the challenges of designing electronics suitable for the space environment, but GPS signal strength and availability in Low Earth Orbit (LEO) is similar to that on Earth. Indeed, GPS navigation for LEO spacecraft has become commonplace [1–5]. The situation is different when the receiver travels in high-altitude orbits above the GPS constellation where GPS signals become sparse and weak. Taking advantage

of signals from the sidelobes of the GPS transmitters can greatly improve signal availability above the constellation, but requires higher sensitivity in the receiver system [6–8].

One approach to increase sensitivity is through the use of special signal processing techniques for weak signals. Significant gains can be achieved in this way, but such weak-signal processing algorithms are often associated with reduced robustness against interference and degraded measurement quality. A complementary and more direct way to increase sensitivity is to gather more signal energy with a high-gain directional antenna. However, if the signals of interest arrive from a wide range of directions, as occurs in the case of GPS, physically pointing a high-gain antenna toward each desired direction becomes impractical. An equivalent result can be achieved with an electronically steered antenna array that does not require a mechanically gimbaled antenna. Such arrays offer advantages beyond simple single-lobe directivity in that they provide the potential to synthesize multiple beams in which gain is optimally distributed toward desired signals and away from interferers.

This paper presents preliminary results in the development and test of a digitally-steered antenna array for the high-altitude Navigator space GPS receiver program at the Goddard Space Flight Center (GSFC) of the National Aeronautics and Space Administration (NASA). We refer to this project as the Navigator GPS Digital Beam Former (NavDBF). The next section gives a background about the Navigator program, followed by a brief review of antenna arrays and beamforming. Next, the GPS signal simulator and the three beamforming methods implemented in this project (a traditional deterministic beamformer and two adaptive optimization-based methods) are described in detail. The results of beamforming simulations and tests are presented and discussed. A summary of the project and possible future work concludes this paper.

NASA GSFC'S NAVIGATOR GPS RECEIVER PROGRAM

NASA GSFC's Components and Hardware Systems branch has been developing GPS receivers for space since the mid 1990s. Early receivers used commercial GPS chipsets and were tested on balloon experiments and in space-GPS research [6], including extending space-based GPS to high altitude missions above the GPS constellation itself [6, 8, 9]. At this altitude, signals are sparse and weak (see Figure 1). This research suggested the need for a specialized receiver designed with high-altitude applications in mind, and so was born the Navigator GPS program.

The current-generation Navigator receiver, which achieves its high sensitivity through signal processing techniques, provides excellent performance in many high altitude applications [7, 8]. This capability led NASA to select Navigator as the onboard GPS receiver for the highly-elliptic Magnetospheric Multiscale (MMS) mission [8, 10], for which we have built and delivered eight flight-qualified receivers. Besides MMS, Navigator receivers have been built for the Global Precipitation Measurement (GPM) mission and an orbital demonstration during the Hubble Space Telescope Servicing Mission 4 (HST-SM4). The weak-signal capability of the Navigator GPS receiver has led to its use in numerous mission studies, such as the Geostationary Operational Environmental Satellite (GOES) and Orion reentry. The Navigator technology has also been commercialized and is used in the receiver for the Orion Crew Return Vehicle and a GPS receiver product developed by Broad Reach Engineering.

NASA has continued to increase the performance of the Navigator GPS receiver through Internal Research and Development (IRAD) funding. The next-generation Navigator receiver will increase sensitivity by at least a factor of 10 to about 15 dB-Hz, improve performance in the presence of interference, and include support for modern GPS signals such as L2C and L5. The use of a

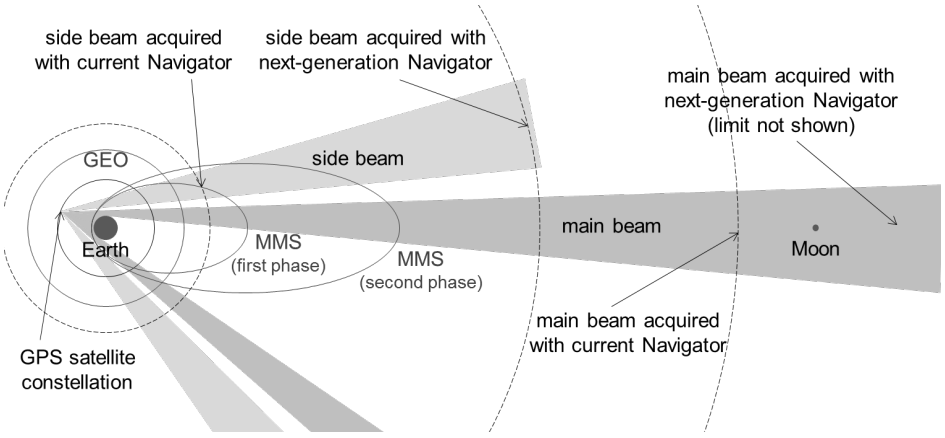

Figure 1: Regions of visibility of the GPS satellites. The dashed lines represent the approximate limits below which the side and main beams of a GPS satellite can be acquired by a GPS receiver sensitive to 25 dB-Hz (current Navigator capability) and 15 dB-Hz (proposed next-generation Navigator). The Geosynchronous Earth Orbit (GEO) and the two phases of the MMS mission orbit are shown for comparison.

digitally-steered antenna array attempts to meet the first two of the these three goals and is the focus of the NavDBF project.

Navigator Technology Development and Implementation Plan

The Navigator GPS team has developed a three-stage technology advancement process to mature future Navigator GPS technologies from concept to flight (see Figure 2). This process defines a chain of three hardware platforms, which interface to low-level signal processing routines via an abstracted hardware layer and allows the flight software (with MMS and GPM Technology Readiness Level (TRL) 8 heritage) to be common among all three development stages.

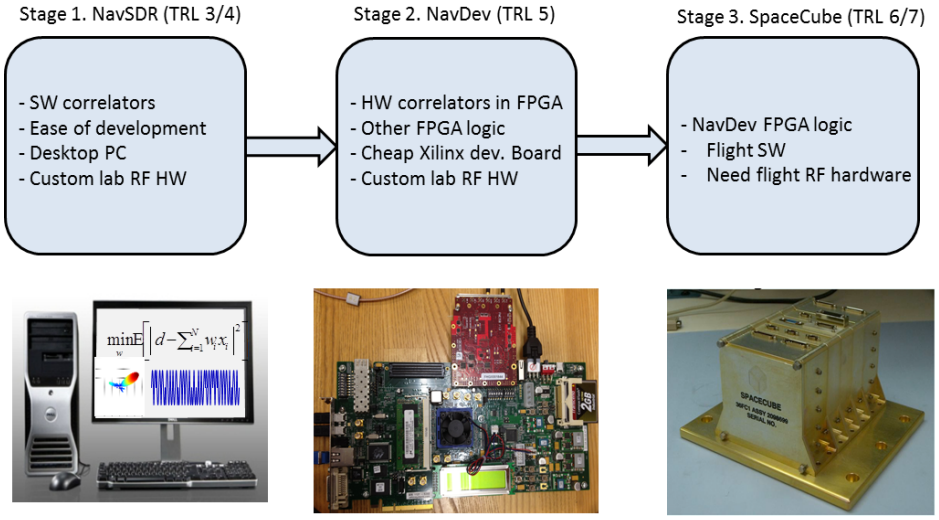

Figure 2: Three-stage navigator GPS technology development process

In the first stage of development, new algorithms and other technologies are implemented in our PC-based real-time Software Defined Radio (SDR) called the Navigator SDR (NavSDR). The

NavSDR provides flexibility and ease in developing and testing new algorithms, but is furthest from being flight-ready. Making the transition from stage one to two involves porting signal processing enhancements from the NavSDR software to the Very High Speed Integrated Circuits (VHSIC) Hardware Description Language (VHDL) for implementation on a Field Programmable Gate Array (FPGA). Our second stage platform, which we call the Navigator GPS Development Platform (NavDev) is based on a commercial FPGA development board (Xilinx ML605) and uses flight heritage firmware from the FPGA-based Navigator GPS receiver. This stage provides a low-cost, high-performance platform that is a short step away from flight. The third and final stage is a Xilinx Virtex 5 based flight avionics platform (GSFC's SpaceCube). The transition from stage two to three involves re-targeting the firmware for a slightly different FPGA family and replacing the laboratory Radio Frequency (RF) front-end hardware with flight electronics. The three stages of development correspond, roughly, to TRL levels 3-4, 5, and 6-7, respectively [11].

The plan for the development of the NavDBF was to build a 16-element antenna array[1] and front-end and implement digital beamforming algorithms in the stage one NavSDR platform. We planned to test the receiver with both live-sky and simulated GPS signals. A parallel effort to develop an array signal simulator in MATLAB, to produce simulated sampled data from an array and array front-end, was undertaken in order to test our beamforming algorithms before the fabrication of the front-end was completed.

ANTENNA ARRAYS AND BEAMFORMING

Antenna arrays have been extensively used in communication and radar systems that may be subject to intentional and unintentional interference. Adaptive antenna arrays were introduced in the early 1960s to obtain antenna directivity (see [12, 13]). The adaptivity in these antennas was achieved using a set of phase-locked loops to adjust the phases of each of the antenna elements relative to a reference signal.

There are many different algorithms that have been used for adaptive electronic steering of antenna arrays. Two popular algorithms are the Least Mean Squares (LMS) and Minimum Variance Distortionless Response (MVDR) methods. The adaptive LMS method was introduced by Widrow and Hoff in 1960 [14] and subsequently applied to antenna arrays by Widrow in [15] and has been extensively used in various applications including radar, communication, and control systems. The MVDR adaptive algorithm was introduced by Capon in 1969 [16] where it was used to combine the output of an array of sensors for seismic applications. Both the LMS and MVDR adaptive algorithms have been, and continue to be, extensively used in various applications [17, 18]. In particular, for applications where the direction of the desired signal is not known *a priori* and the characteristics of the noise and the direction of interference are not completely known, adaptive methods have the potential to be far superior to conventional methods that produce fixed antenna patterns [17, 18].

Array signal processing has been applied to GPS receivers for interference mitigation (e.g., [19–28]). Moelker et al. [19], for example, considered adaptive antenna arrays and compared various algorithms and array structures. In [21], Brown and Gerein demonstrated sensitivity gain and interference mitigation in a research GPS array receiver. Lorenz and Boyd [22] demonstrated that a GPS antenna array can be used to mitigate multipath and interference errors using an algorithm based on angle of arrival differences. Kalyanaraman and Braasch [27] integrated an

[1]The choice of a 16-element array provides the next-generation Navigator's target of 10 dB sensitivity gain, and more practically, was the largest array we could afford to build at the time.

adaptive array with a software GPS receiver and studied the effect of narrow band as well as wide band interferences on code and carrier tracking. An overview of GPS interference mitigation techniques including spatial and temporal adaptive filtering methods can be found in [29].

GPS ARRAY SIGNAL SIMULATOR

In order to study various beamforming algorithms, we developed a MATLAB-based GPS simulator that generates signals coming from an antenna array and allows for testing of many different orbital scenarios and algorithms. The simulator obtains position and velocity of the GPS satellites from stored ephemerides and uses them to calculate the L1 Coarse/Acquisition (C/A) GPS signals as received by each element of an antenna array. The simulator can also introduce near-far and multipath interference at the discretion of the user. This section provides some detail on the signals generated by the simulator.

We represent the GPS L1 signal at the transmitter at GPS time t as (assuming zero initial phase)

$$s_T(t) = \sqrt{2P}b(t)\cos\omega_0 t, \tag{1}$$

where P is the power of the transmitted signal, $\omega_0 = 2\pi f_0$, where f_0 is the GPS L1 frequency of 1.57542 GHz, and $b(t) \equiv c(t)d(t)$ is the real baseband signal comprised of the binary $\{+1, -1\}$-valued GPS C/A code signal $c(t)$ and data message $d(t)$. The code $c(t)$ is a 1ms-periodic length-1023 Pseudo-Random Number (PRN) sequence designed to have strong auto and cross-correlation properties, which are critical for precision ranging and Code Division Multiple Access (CDMA). The data $d(t)$ is a 50Hz binary data modulation whose transitions are synchronous with the first transition of the 1ms code [30].

The signal is modeled as being transmitted from the GPS satellite to a receiving antenna through a free-space channel model that currently ignores the effect of the ionosphere and atmosphere. The channel model attenuates the signal to power level C, delays it by $\tau(t)$ and adds bandpass White Gaussian Noise (WGN) $n_0(t)$ with constant spectral density $N_0/2$ over the signal bandwidth.[2] Here $\tau(t) = r(t)/c$ where $r(t)$ is the distance from transmitter at transmit time $t - \tau(t)$ to receiver at receive time t, and c is the speed of light in vacuum. The signal received at the antenna at time t is

$$s_R(t) = \sqrt{2C}b(t-\tau)\cos\omega_0(t-\tau) + n_0(t). \tag{2}$$

The model for the receiver RF front-end filters, amplifies, and down-converts the signal and noise. The filters pass the signal, but limit the noise to bandwidth B. A quadrature down-conversion process mixes the signal with the Local Oscillator (LO) generated tone $e^{-j\omega_{\mathrm{LO}}t}$ to bring the signal and noise to a lower center Intermediate Frequency (IF) $\omega_{\mathrm{IF}} = \omega_0 - \omega_{\mathrm{LO}}$, after which, low-pass filters remove the resulting high frequency $\omega_0 + \omega_{\mathrm{LO}}$ components. Finally, Automatic Gain Control (AGC) circuits rescale the signal plus noise to an appropriate level for the Analog-to-Digital Converter (ADC) to quantize the data with full precision. The specific value of the rescaling factor

[2] The noise has the *bandpass representation*

$$n_0(t) = n_{\mathrm{I}}(t)\cos\omega_0 t - n_{\mathrm{Q}}(t)\sin\omega_0 t$$

with baseband in-phase and quadrature components n_{I}, n_{Q} and $\tilde{n}(t) = n_{\mathrm{I}}(t) + jn_{\mathrm{Q}}(t)$ is the complex envelope of n_0, defined by $\tilde{n}(t) = (n_0(t) + j\hat{n}_0(t))e^{-j\omega_0 t}$ and $\hat{n}_0(t)$ is the Hilbert transform of $n_0(t)$ [31]. In reality, this noise is primarily generated in the first amplifier of the receiver which also greatly amplifies the signal, effectively fixing the C/N_0 for all further processing. It is standard modeling practice to attribute this noise to the channel.

is inconsequential for the model, so we take it to be $\frac{2}{\sqrt{N_0 B}}$, which conveniently normalizes the noise power. Defining the notation $\gamma \equiv C/N_0$ and $\sigma \equiv \sqrt{N_0 B}$, the resulting model at the input to the ADCs is

$$\begin{aligned} s_{\mathrm{IF}}(t) &= s_R(t) 2\sigma^{-1} e^{-j\omega_{\mathrm{LO}} t} \\ &= \sqrt{(2\gamma/B)}\, b(t-\tau)\cos\omega_0(t-\tau)e^{-j\omega_{\mathrm{LO}} t} + 2\sigma^{-1} n_0(t) e^{-j\omega_{\mathrm{LO}} t} \\ &= \sqrt{(2\gamma/B)}\, b(t-\tau) e^{j(\omega_{\mathrm{IF}} t - \omega_0 \tau)} + \sigma^{-1}\tilde{n}(t) e^{j\omega_{\mathrm{IF}} t} \\ &= s(t) + n(t). \end{aligned} \tag{3}$$

where $\tilde{n}(t)$ is the complex envelope of $n_0(t)$ (see Footnote 2 or [31]) and $n(t)$ is then complex bandpass WGN noise centered at ω_{IF} with independent unit variance real and imaginary components.

The signal plus noise is then sampled to get $x^k = x(t^k)$ at the regular sampling times $t^k = kT_s + t_0$, for k a positive integer, and t_0 an arbitrary starting time. In our simulation, we assume that $T_s = 1/B$. The advantage of this assumption is that the simulated noise is then uncorrelated from sample to sample. Finally, we arrive at the IF sampled data model

$$\begin{aligned} x^k &= Q[s^k + n^k], \\ s^k &= \sqrt{(2T_s\gamma^k)}\, b(t^k - \tau^k) e^{j(\omega_{\mathrm{IF}} t^k - \omega_0 \tau^k)}. \end{aligned} \tag{4}$$

where $Q[\cdot]$ is the quantization function.

The GPS signal simulator generates files of complex x^k samples for a variety of configurable input parameters including the bits of precision for the quantizer $Q[\cdot]$, ω_{IF}, T_s, $\gamma(t)$, and $\tau(t)$. The model (4) provides the correct IF signal structure for any GPS receiver with matching configuration values of ω_{IF}, T_s, etc., to acquire and track the sampled data.

Higher level GPS processing, e.g., solving for position, velocity and time, requires multiple signals from different transmitters. Each signal must have $d(t)$ and $\tau(t)$ consistently modeled in accordance with GPS-IS-200 [30] to account for transmitter and receiver dynamics. The most direct way to model multiple transmitters consistently is to take stored GPS ephemerides and almanac data from Internet archives and compute transmitter states according to the algorithms outlined in the GPS-IS-200.

The simulation must simultaneously reconstruct the $d(t)$ using the ephemeris and almanac data along with simulation time information. Our receiver also models the receiver dynamics based on simple earth-orbital or random-walk dynamics. Once the transmitter/receiver (tx/rx) dynamics are established, the signal parameters can be calculated. Since the dynamics are very smooth the tx/rx states and signal parameters τ and γ can be calculated at a relatively low rate (1 ms in our simulator) with simple interpolation used to determine $\tau(t^k)$ and $\gamma(t^k)$ at every sampling time.

To model the signals from a constellation of M GPS transmitters received by an N-element array, we can use the single tx/rx model (4) separately $M \times N$ times. We annotate s, τ and γ with two indicies, i and j, to represent the path from transmitter i to array element j. The combined signal received by array element j can then be modeled as

$$\begin{aligned} x_j &= s_j + n_j, \\ s_j &= \sum_{i=1}^{M} s_{ij} = \sum_{i=1}^{M} \sqrt{(2T_s\gamma_{ij})}\, b_i(t-\tau_{ij}) e^{j(\omega_{\mathrm{IF}} t - \omega_0 \tau_{ij})}, \end{aligned} \tag{5}$$

where index i is summed over since the transmitted signals are received additively, and n_j is an independent additive noise term for each array element. We have omitted the quantization operation and the sampling superscript k here to simplify notation.

Two approximations can be used to simplify the model (5). The first is based on the assumption that the array is much smaller than the transmit-to-receive path lengths, i.e., $\|\mathbf{p}_j\| \ll r_{ij}$, for all i, j, where $\mathbf{p}_j$ is the position offset of the jth array element relative to reference element 0. This assumption allows the approximation $\tau_{ij} \approx \tau_{i0} + \mathbf{k}_i^{\mathrm{T}}\mathbf{p}_j/\omega_0$, where $\mathbf{k}_i$ is the propagation vector from transmitter i to the array. Second, under the assumption that that modulation envelope changes negligibly in the time it takes the signal to propagate across the array, sometimes called the *narrowband condition*, we have $b_i(t - \tau_{ij}) \approx b_i(t - \tau_{i0})$. Together, these approximations, both valid in our case, give the signal at the jth element as

$$\begin{aligned} s_j &\approx \sum_{i=1}^{M} \sqrt{(2T_s\gamma_{ij})} b_i(t - \tau_{i0}) e^{j(\omega_{\mathrm{IF}} t - \omega_0 \tau_{i0} - \mathbf{k}_i^{\mathrm{T}}\mathbf{p}_j)} \\ &= \sum_{i=1}^{M} s_{i0} h_{ij}, \text{ with } h_{ij} \equiv e^{-j\mathbf{k}_i^{\mathrm{T}}\mathbf{p}_j}. \end{aligned} \tag{6}$$

Under these approximations, the signal received from the ith transmitter by each array element is related to that received by one reference element by a simple phase shift h_{ij}. We refer to these phase shifts as the *geometric phase shifts* since they are defined only by the geometry of the transmitters and array elements. In the traditional beamformer described below, the complex conjugates of these phase shifts are used as weights in combining the array signals. The effect is that the signals are added coherently, giving maximal gain in direction of each transmitter. See Figure 3.

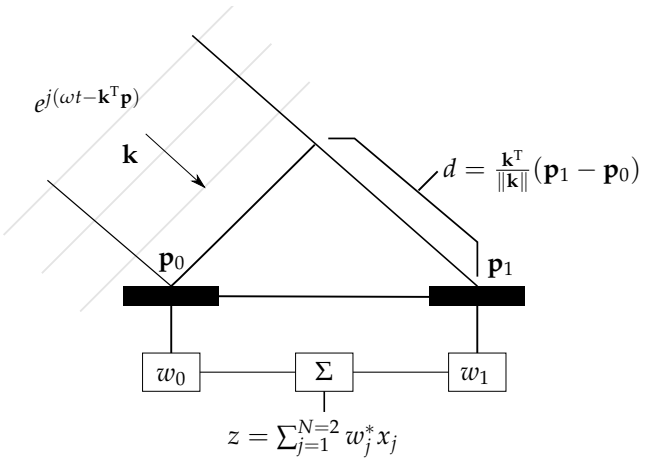

Figure 3: Array geometry for a two-element array.

In summary, the software array signal simulator, which was used for testing several beamforming methods, works in the following three step process:

1. Simulate transmitter and receiver dynamics (including attitude dynamics for the latter) at low rate time steps (nominally 1 ms). Determine signal parameters $\tau_{ij}(t), \gamma_{ij}(t)$, as a function of the tx/rx dynamics or otherwise, as directed by input options.

2. Interpolate signal parameters to sampling times.

3. Compute (5) (with approximations used in (6)) and store the result to a file.

To simplify implementation and analysis, the following assumptions were used in the simulator. Transmitter and receiver clock errors, ionospheric delay, and dispersive atmospheric effects were not modeled. Also, to allow for easy modeling of interference and multipath, carrier-to-noise density ratio levels were defined by user-specified profiles rather than based on a tx/rx link model.

Modeling Near-Far Interference and Multipath

One goal of this work is to demonstrate the utility of the array in mitigating two important interference effects: near-far interference (where the receiver attempts to process weak signals in the presence of much stronger GPS signals) and multipath (where receiver collocated physical structures provide reflection paths which cause a delayed version of the signals to appear at the antenna). Multipath can be one of the dominant sources of error for a GPS receiver as it can compromise the ability to make precise range measurements.

Since the simulator accepts user specified C/N_0 profiles, near-far interference can be generated by including weak and strong signals simultaneously. Differences higher than around 24 dB are known to exceed the natural cross-correlation protection of the C/A code [32]. Multipath signals can be modeled in the simulator by replicating the transmitter signals seen by the receiver with additional delays, from different directions of arrival, and adding them.

ARRAY SIGNAL PROCESSING ALGORITHMS

The elements of an antenna array sample incident signals in the space domain like analog-to-digital converters sample signals in the time domain. Likewise, array signal processing techniques allow for the synthesis of spatially selective filters (in $\mathbf{k}$ space) that condition and extract information while reducing noise and interference, which is analogous to the synthesis of frequency selective filters (in ω space) in Discrete-Time Signal Processing (DTSP) that do the same. While there are many different ways to combine the array data [33], there exists a simple, yet fundamental, class of algorithms that are mathematically similar to the ubiquitous N-tap Finite Impulse Response (FIR) filter of DTSP. These algorithms multiply the input signals x_j by complex weight w_j and sum over the N elements,

$$z = \sum_{j=1}^{N} w_j^* x_j = \mathbf{w}^{\mathrm{H}} \mathbf{x}, \tag{7}$$

where the asterisk * denotes complex conjugate and superscript $^{\mathrm{H}}$ denotes Hermitian (complex conjugate transpose). Note that the array output and weight vector have been represented by column vectors and the index i has been removed to simplify notation. We restrict attention to this class of methods in our investigation.

The *beam pattern* corresponding to a given weight vector $\mathbf{w}$,

$$B(\mathbf{k}) \equiv \sum_{j=1}^{N} w_j^* e^{-j\mathbf{k}^{\mathrm{T}} p_j}, \tag{8}$$

summarizes the response of the array to incident plane waves (exactly) and narrowband signals $f(t)$ (approximately): the response to $x(t) = f(t)e^{j(\omega t - \mathbf{k}^{\mathrm{T}}\mathbf{p})}$ is $B(\mathbf{k})f(t)e^{j\omega t}$. By control of the array

weights, the array's beam pattern can be optimized to achieve certain desirable characteristics including: directivity, signal-to-noise ratio gain, and interference mitigation. This optimization can be done with statically fixed weight designs or with dynamically adaptive algorithms where the performance index evolves with the signal and interference environment over time. If the optimization can converge faster than the objective changes, then performance goals can likely be met.

Digital vs. Analog Beamforming

One should note that the input $\mathbf{x}$ in (7) could equally well be a continuous-time analog signal, or a discrete-time digital signal. While analog and digital beamforming can achieve the same goals in principle, the digital approach has the advantage that the associated front-end captures all relevant information available to the array. Thus, the flexibility of modern re-programmable digital logic and high speed computers can be used to implement and evaluate different array-processing algorithms. Analog beamformers have reduced computational requirements, however, and may be the only option for wideband signals, where digital sampling rates required for the digital approach may become prohibitively high.

Traditional Beamformer

The traditional beamformer uses the weights

$$w_j = \frac{1}{N} e^{-j\mathbf{k}_0^{\mathrm{T}}\mathbf{p}_j} \tag{9}$$

for element j, where $\mathbf{k}_0$ is the wave vector of the signal of interest and $\mathbf{p}_j$ is the position of antenna j. Since these weights are precisely the geometric phase shifts, defined in (6), it is clear that (under the narrowband assumption) the different signals from the array will be combined coherently. Also from (8), $B(\mathbf{k}_0) = 1$. Since the signal then adds coherently, and the noise incoherently, the Signal-to-Noise Ratio (SNR) gain of the signal received along direction $\mathbf{k}_0$ is N: this is the best that can be done in terms of pure SNR gain [33].

Phase compensation in the traditional beamformer is the simplest of the tested beamforming methods. This algorithm is not adaptive and it requires prior knowledge of the geometry of the array $\mathbf{p}_j$ and the direction of the signal of interest $\mathbf{k}_0$. While it can steer the main beam of the array pattern to that direction and has reduced gain elsewhere, which can help against interference, it does not actively control its sidelobe or null structure.

Optimization Based Methods

Minimum Mean Square Error (MMSE) beamformers minimize the mean square error of the combined inputs from the antenna array with respect to a reference signal r. The popular Least Mean Squares (LMS) algorithm was implemented in the NavSDR to solve the MMSE problem

$$\min_{\mathbf{w}} \mathrm{E}[|r - \mathbf{w}^{\mathrm{H}}\mathbf{x}|^2]. \tag{10}$$

In our investigation, the reference signal r was set to be the locally generated GPS carrier spread by the unique C/A code for each GPS satellite. The LMS algorithm creates a beam pattern that points toward this satellite, without requiring prior knowledge of the direction of arrival of the transmitted signal.

Minimum Output Energy (MOE) beamformers minimize the total output energy except in the direction of the transmitter. One example which was tested in simulation is the Minimum Variance Distortionless Response (MVDR) beamformer. The algorithm selects the weight vector $\mathbf{w}$ such that the variance of the combined signals from the antenna array is minimized, subject to the constraint that the signal power is fixed in the desired look direction where $\mathbf{h}$ is the vector of elements $h_j = e^{-j\mathbf{k}_0^T \mathbf{p}_j}$. Formally, it attempts to solve

$$\min_{\mathbf{w}} \mathrm{E}[|\mathbf{w}^H \mathbf{x}|^2], \quad \mathbf{w}^H \mathbf{h} = 1, \tag{11}$$

(Note, referring to (8), that $\mathbf{w}^H \mathbf{h} = B(\mathbf{k}_0)$.) Under this constraint, the algorithm requires knowledge of the direction of the signal of interest, but not of the direction of interference.

The MVDR and LMS algorithms were implemented in the NavSDR according to the method described in [25]. For both methods, the step size parameter of the update equations were chosen by stability criteria shown in [18] and also to find the ideal balance between settling time and mean error. In future work, these parameters will need to be adjusted to remove their dependence on input signal power.

Comparison of Beamforming Algorithms

Traditional beamforming is the simplest of the three methods studied and has the lowest computational cost. However, to implement this method, and any other that explicitly points the array in a certain direction (including MVDR), requires knowledge of the array attitude and calibration data to correct for inter-element phase differences due to hardware. Table 1 summarizes many of the trade-offs between the three beamforming methods studied. As an example, Figure 4 illustrates the simulated response of the LMS and MVDR methods in the presence of multipath interference. With the MVDR method, the main beam is centered on the signal of interest while the side beams are steered away from the interfering signals as much as possible for the geometry of this simulation. With the LMS method, in this simulation, the side beams are steered toward the multipath signals. In theory, there are some conditions under which LMS will mitigate the multipath signals, including when the SNR is lower than the SNR of the desired signal and when the update equation is properly tuned to the dynamics of the signal environment.

The three beamforming methods studied were implemented in a MATLAB tracking program for initial verification, and later in the NavSDR. It was observed that an important modification to the

Table 1: This table summarizes the advantages and disadvantages of implementing, in a GPS receiver, the three beamforming methods presented in this paper. The best method to use (highlighted in gray) varies depending on knowledge of the direction of the signals of interest and availability of processing power.

Beamforming Method	**Traditional**	**LMS**	**MVDR**
Calculation	direct	iterative	iterative
Computation cost	low	high	high
Requires known direction of signal of interest	yes	no	yes
Requires calibration	yes	no	yes
Reduces near-far interference	may	yes	yes
Reduces interference from multipath signals	may	may	yes

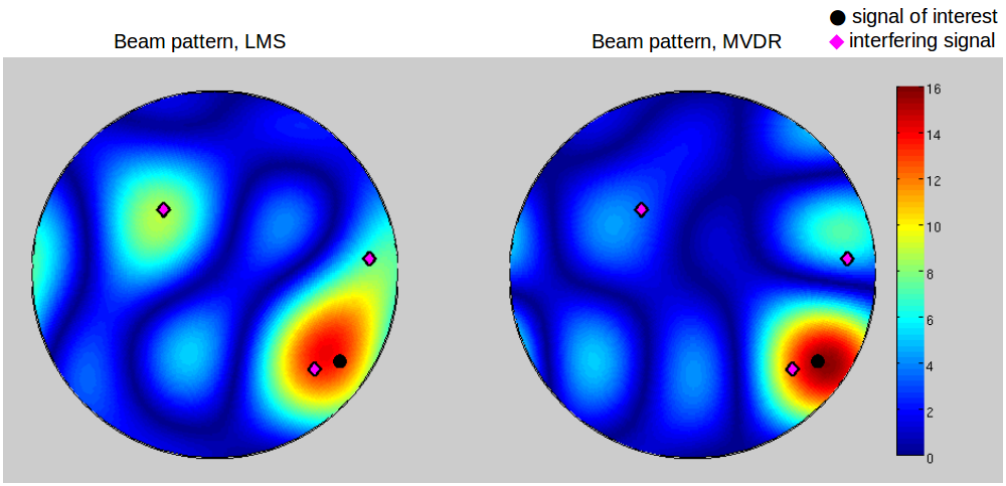

Figure 4: Simulated hemispherical beam pattern, as seen from above, of an antenna array with 16 elements, in the presence of multipath signals.

LMS method was necessary due to the GPS signal structure. The LMS method requires a known reference signal, but since the GPS binary data is unpredictable, the algorithm was modified to become insensitive to the bit transitions in the data. Without this modification, the method becomes unstable.

DESIGN OF ARRAY AND ARRAY FRONT-END

An antenna array was designed and fabricated using inexpensive GPS L1 patch antennas and characterized in one of Goddard's anechoic chambers. The array consists of 16 elements with equal horizontal and vertical spacing between antennas, in a 4x4 grid. The spacing is half of the GPS L1 wavelength ($\lambda_{L1}/2$), about 9.5 cm, which is optimal for a regular array with a beam pattern having a single, narrow-as-possible, main beam. The main beam width is inversely proportional to the size of the array and wider spacing than $\lambda_{L1}/2$ leads to multiple main beams or "grating lobes" (analogous to aliasing in DTSP for sampling rates lower than the Nyquist rate).

An array RF front-end was also designed and built for laboratory use, to coherently down-convert and sample each of the signals from the individual array elements. The design is partitioned into a motherboard and 16 daughterboards (each one producing digital samples from one of the antennas). The samples are filtered and packed in an FPGA on the motherboard, which also handles frequency synthesis and hosts the power circuits. Figure 5 shows a diagram of the front-end, and Figure 6 shows an image of the complete motherboard with daughterboards after they were built and assembled.

ARRAY RECEIVER TEST RESULTS

The three beamforming methods were implemented in the NavSDR and tested using both the MATLAB simulated and live-sky signals. In all the live-sky tests our 16-element antenna array and custom front-end were used. Tests of multipath and near-far interference were conducted using the MATLAB simulator since such scenarios are impossible to control with live-sky signals.

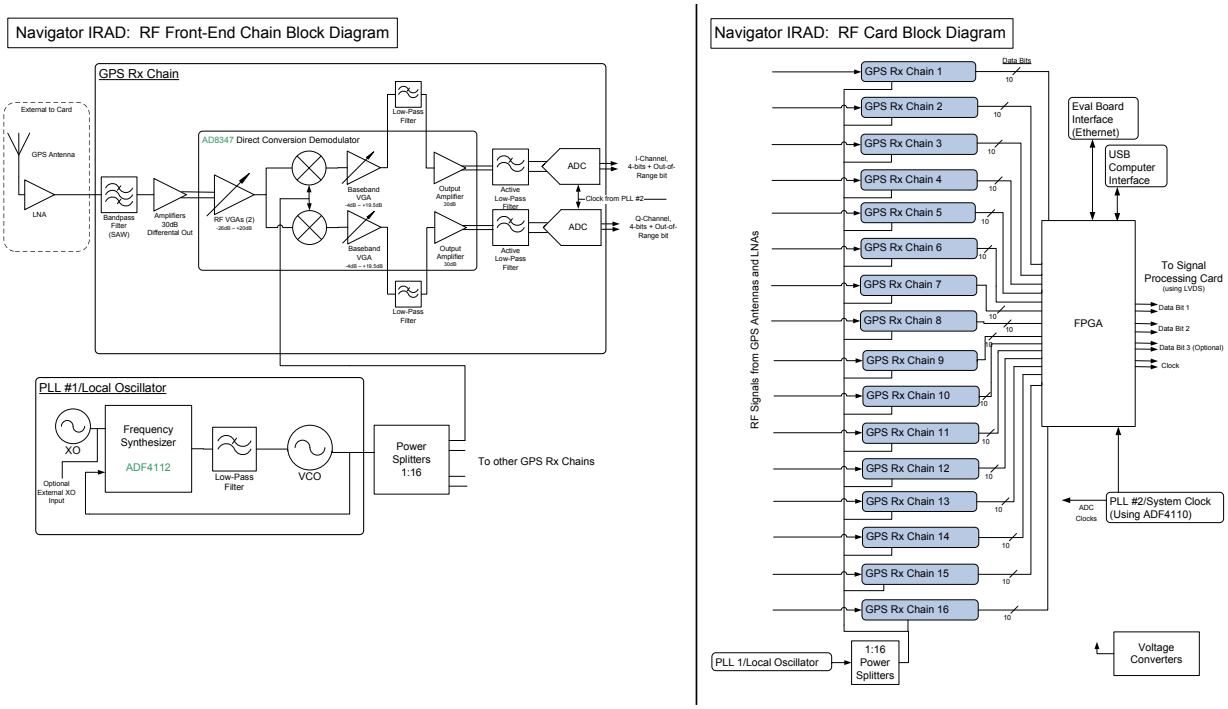

Figure 5: Block diagram of array front-end design.

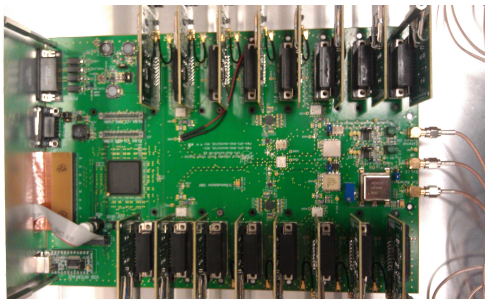

Figure 6: Array front-end motherboard with 16 daughterboards (partially visible) attached

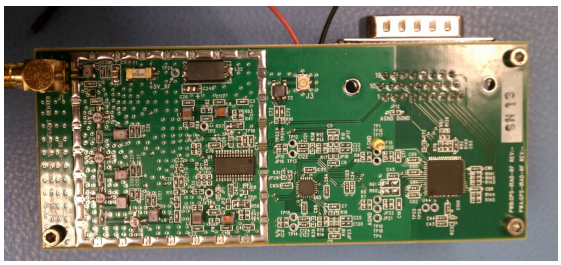

Figure 7: Array front-end single-channel downconversion and digitization daughterboard

Simulated Signals

Single Antenna and Array (Without Interference)

The first test simulated GPS signals received from five satellites, at a fixed $C/N_0 = 45$dB-Hz as seen by a single antenna. This level is typical for a receiver on the Earth's surface. Figure 10a shows the array-receiver estimates of the C/N_0 for the five satellites, first using one antenna and then, after 20 seconds, combining all 16 antennas using the LMS beamforming method. The observed increase in C/N_0 was approximately 12 dB, expected for 16 antennas (as $10\log_{10}16 = 12$ dB). The results using the other two methods showed similar C/N_0 increases. We also studied the effect of the array on the Position, Velocity, Time (PVT) solution quality. The standard deviation of the calculated position was improved from about 14.5 m before beamforming to about 4.5 m afterwards. This error is somewhat higher than expected for the corresponding signal levels and geometry (8.8m and 2.2m, respectively); the reason for this has not yet been identified. Regardless,

the fractional decrease in the error (69%) is close to the expected improvement (75%).

Near-Far Interference Test

To simulate near-far interference, four GPS transmitters were set at a signal level of 35 dB-Hz, and a fifth at 65 dB-Hz. The results in Figure 8 show the C/N_0 for several GPS transmitters in the presence of an interferer. In each scenario, the interference starts 20 seconds into the simulation. Figure 8a shows the signals when they are tracked using one antenna. Once the interference begins, the signals are severely attenuated and several cross-correlations are tracked, causing the PVT solution to be corrupted. In Figure 8b, all the signals from the array are combined using the traditional beamforming method. The gain in the direction of the signals of interest provide some protection against the interferer. The LMS method (Figure 8c) fails in this case. This is not unexpected because the interference exceeds the 24 dB cross-correlation protection level. The interferer and local reference have a strong enough correlation so that the algorithm converges on the interference and not the desired signal. The MVDR method (Figure 8d) improves the gain in the direction of the signal of interest (over the traditional beamformer), as well as reducing interference.

Multipath Test

In this scenario, signals from five GPS transmitters were simulated. For each transmitter, the direct signal and one multipath signal were created, the multipath signal being a replica of the corresponding direct signal with a different delay (20, 40, 60, 80 or 100 meters) and direction of arrival. All signals were simulated with the same C/N_0 of 45 dB-Hz, representing an extreme case of multipath interference. Performance was measured by the effect on the point solution position. As shown in Figure 9, with one antenna, the multipath interference causes a large bias and increased noise level in the calculated position. This result exemplifies the effect of multipath interference in GPS performance: the multipath signals distort the code correlation function, causing bias in the measurements, while also causing destructive interference of the carrier, reducing the C/N_0. With any beamforming method, the C/N_0 is increased, which results in a better PVT solution due to less noise, but not necessarily a lower overall error as the position may still be biased. In this simulation, only the methods based on direction of arrival (the traditional beamformer and MVDR) are able to attenuate the effect of the multipath signals significantly and reduce the overall error.

Live-Sky Signal Tests

Array Calibration

The beamforming methods were also tested with live GPS signals, using our low-cost antenna array. While the simulated data assumes that the phase differences between the antennas are only due to their position and the direction of arrival of the signals, the RF front-end has unequal path lengths, causing additional phase differences between each of the signals from the antennas. These phases have to be calibrated out for the beamforming methods that require a known direction of arrival (traditional beamformer and MVDR). The calibration was done by tracking the signal from the same satellite with all antennas and comparing the phase of the local carrier calculated by the tracking loop of the receiver software. The procedure was repeated for several satellites, and the phase difference due to position of the antennas and direction of arrival was subtracted from

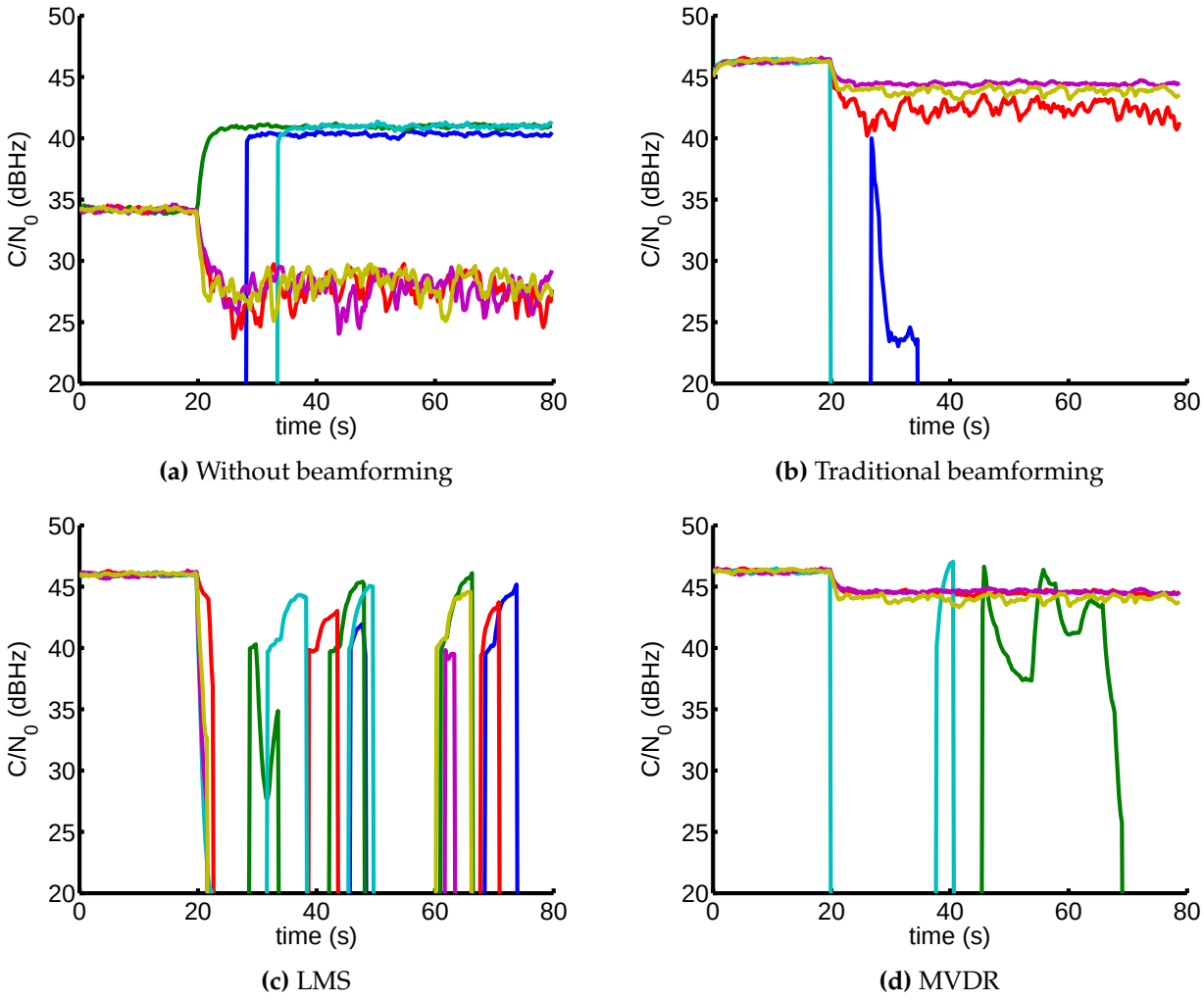

(a) Without beamforming

(b) Traditional beamforming

(c) LMS

(d) MVDR

Figure 8: C/N_0 before and after strong near-far interference begins (20 seconds into the simulation), with and without beamforming. Each trace represents the signal from a different satellite. The interference causes a large decrease in C/N_0 with one antenna (subfigure 8a) and the acquisition and tracking of cross-correlated signals. The 65 dB-Hz interferer is not tracked because the signal power is too high for the NavSDR (certain calculations overflow and fail). Traditional beamforming (8b) and MVDR (8d) reduce the effect of the interference. In each case, there is only a small decrease in C/N_0 and cross-correlated signals are avoided. LMS (8c) is not able to maintain track of any signal in this case.

the total phase difference from the local carrier. The remainder was approximately constant, and assumed to be the bias.

Single Antenna and Array (Without Interference)

The receiver test results in Figure 10b show C/N_0 estimates for five satellites initially using only one antenna, and after 60 s, combining the signals from all of the antennas using the LMS method. The increase in C/N_0 upon turning on the array was about 11 dB on average, close to the expected 12 dB of gain for 16 antennas. Unlike in the simulations, the increase in C/N_0 varied depending on the satellite, probably due to the varying sensitivities of the antennas for different directions of arrival. Also, the initial C/N_0 estimates are somewhat lower than expected for live-sky signals.

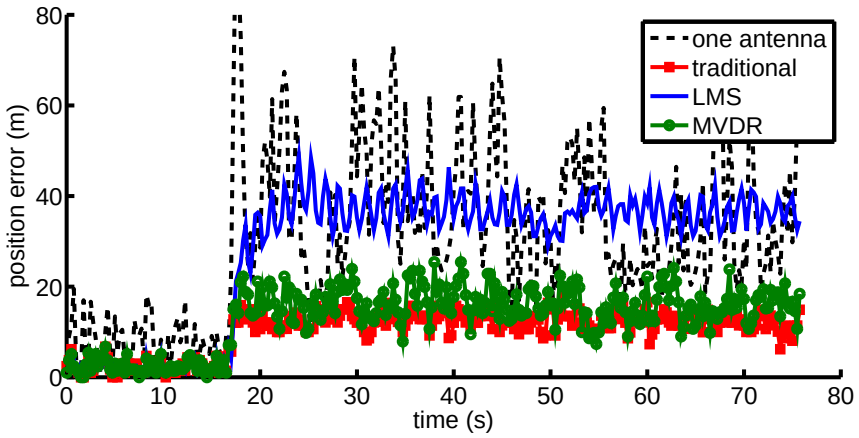

Figure 9: Error in position calculation in the presence of multipath interference. Multipath signals start at about 17 seconds. LMS reduces the variance in the calculated position, but not the bias. Traditional beamforming and MVDR reduce the overall error caused by multipath signals.

This loss is attributed to issues with the array front-end which are still under investigation. As expected, the error in the position calculated by the receiver decreased with the increase in C/N_0. The standard deviation of the calculated position was improved from about 14 m before beamforming to about 5 m afterwards. These levels are consistent with our earlier investigation using simulated signals, presented above.

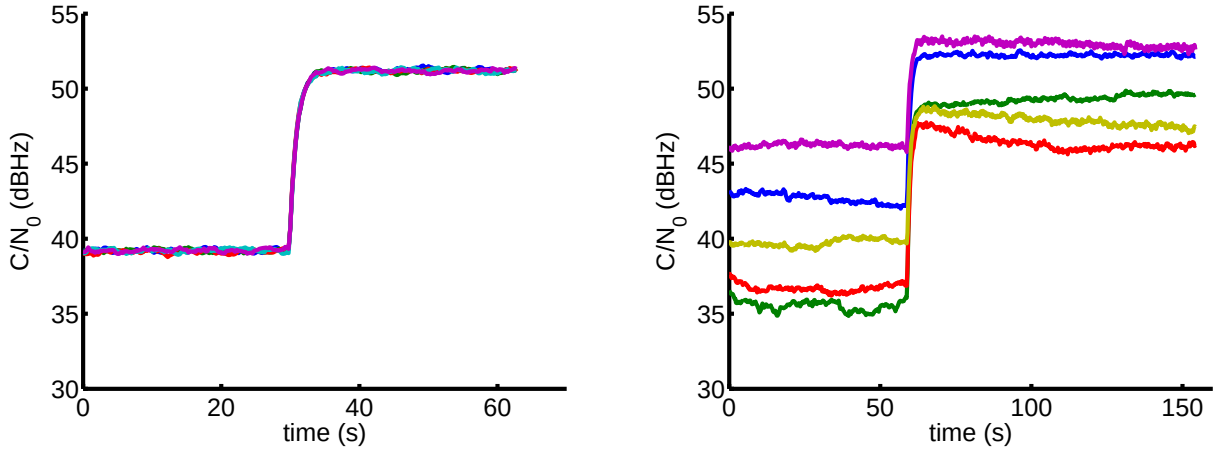

(a) Simulated signals

(b) Live signals

Figure 10: C/N_0 of GPS signals before and after beamforming. The increase is close to the ideal value (12 dB for 16 antennas).

CONCLUSIONS AND FUTURE WORK

In this paper, we presented preliminary results from the Navigator GPS Digital Beam Former (NavDBF) technology development project. The paper described the design and development of a 16-element antenna array and front-end electronics, the development of a MATLAB-based GPS signal simulator, the evaluation and implementation of one fixed and two adaptive algorithms for Digital Beam Forming (DBF) in both a simple off-line MATLAB GPS receiver simulation and

our NavSDR real-time software GPS receiver development platform, and finally the assembly of a complete GPS receiver with beamforming capability. Promising initial results were presented, using both simulated and live-sky GPS signals, which largely demonstrated the expected gains in sensitivity and interference mitigation for both near-far and multipath interference.

Future work will focus on pushing the NavDBF along the standard three-stage technology development process, which was also introduced in this paper. The next stage in the process involves porting the algorithms from the NavSDR to the NavDev FPGA platform. We are also developing a flight-qualified, miniaturized, RF front-end. A GSFC IRAD proposal was selected to begin this work, which will leverage a related NASA Phase II Small Business Innovation Research (SBIR) contract that is funding the development of a multichannel GPS front-end Application Specific Integrated Circuit (ASIC).

Future Applications for NavDBF

The NavDBF has potential application to missions whose attitude dynamics do not allow for a permanent zenith (for LEO) or nadir (for GEO) pointed GPS antenna, and who may, therefore, have some difficulty maintaining good GPS coverage with fixed body-mounted antennas. It also has application to missions that need high precision in PVT measurements in a poor multipath environment such as on the International Space Station (ISS), specifically the multipath mitigation benefit.

The MMS mission, in its highly-eccentric, high-altitude orbits, and use of four spacecraft in formation, represented an ideal target application for the Navigator GPS receiver. In addition to the weak signal environment, physical constraints on the spacecraft design forced the use of an array of four GPS antennas placed around the perimeter of the spacecraft. As the four MMS spacecraft rotate (at 3 revolutions per minute), the receiver maintains continuous GPS tracking by switching from one antenna to the next in sequence. This switching mechanism works well enough to meet mission requirements but has performance costs relative to an omnidirectional antenna. A beamforming approach, which would combine the array of signals, would have more gain and allow for smoother tracking of the signals during spacecraft rotation. This approach could be applied to future missions with similar challenges.

An interesting example application of NavDBF is a hypothetical Geosynchronous Earth Orbit (GEO) spacecraft-servicing mission that would need to maneuver around a GEO target spacecraft and may not be able to support a nadir-pointed or gimbaled high-gain GPS antenna. Such a mission would benefit greatly from an array of GPS antennas that could be optimally combined. For such a mission, the potential application of NavDBF goes beyond just providing effective GPS navigation. The NavDBF could provide a sensor capability for Automated Rendezvous and Docking (AR&D) operations by tracking GPS signals reflected from the target spacecraft and measuring their angle of arrival and range to target. The Navigator team has investigated this type of application during HST-SM4 and is currently actively involved in continuing this research.

REFERENCES

[1] L. Carson, L. Hailey, G. J. Geier, R. Davis, G. Huth, and T. N. Munson, "Design and predicted performance of the GPS demonstration receiver for the NASA TOPEX satellite," in *Position Location and Navigation Symposium*, pp. 442–454, IEEE, 1988.

[2] G. H. Born, M. E. Parke, P. Axelrad, K. L. Gold, J. Johnson, K. W. Key, D. G. Kubitschek,

and E. J. Christensen, "Calibration of the TOPEX altimeter using a GPS buoy," *Journal of Geophysical Research*, vol. 99, no. C12, pp. 24517–24, 1994.

[3] P. Kachmar, W. Chu, P. Neirinckx, and M. Montez, "US Space Shuttle: Integrated GPS navigation capability," in *Proceedings of the 6th International Technical Meeting of the Satellite Division of The Institute of Navigation*, pp. 313–326, 1993.

[4] K. Gold, A. Reichert, G. Born, W. Bertiger, S. Wu, and T. Yunck, "GPS orbit determination in the presence of selective availabilty for the Extreme Ultraviolet Explorer," in *ION GPS-94*, pp. 1191–1199, 1994.

[5] "Gravity Recovery and Climate Experiment." http://science.nasa.gov/missions/grace/. Retrieved Sept 24, 2012.

[6] M. Moreau, *GPS Receiver Architecture for Autonomous Navigation in High Earth Orbits*. PhD thesis, University of Colorado, Boulder, 2001.

[7] W. Bamford, L. M. B. Winternitz, and M. Moreau, "Navigation performance in high earth orbits using navigator GPS receiver," in *29th Annual Guidance and Control Conference, Breckenridge, CO*, 2006.

[8] L. M. B. Winternitz, W. A. Bamford, and G. W. Heckler, "A GPS receiver for high-altitude satellite navigation," *IEEE Journal of Selected Topics in Signal Processing*, vol. 3, no. 4, pp. 541–556, 2009.

[9] M. Moreau, P. Axelrad, J. Garrison, M. Wennersten, and A. Long, "Test results of the pivot receiver in high earth orbits using a GSS GPS simulator," in *Proceedings of the Institute of Navigation GPS Conference*, 2001.

[10] T. Lulich, W. A. Bamford, L. B. W. Winternitz, and S. R. Price, "Results from Navigator GPS flight testing for the Magnetospheric Multi Scale (MMS) mission," in *ION GNSS*, 2012.

[11] J. C. Mankins, "Technology readiness levels: A white paper," tech. rep., NASA, Office of Space Access and Technology, Advanced Concepts Office, 1995.

[12] R. Ghose, "Electronically adaptive antenna systems," *IEEE Transactions on Antennas and Propagation*, vol. 12, no. 2, pp. 161–169, 1964.

[13] J. Eberle, "An adaptively phased, four-element array of thirty-foot parabolic reflectors for passive (echo) communication systems," *Antennas and Propagation, IEEE Transactions on*, vol. 12, no. 2, pp. 169–176, 1964.

[14] B. Widrow and M. E. Hoff, "Adaptive switching circuits," pp. 96–104, 1960.

[15] B. Widrow, P. E. Mantey, L. J. Griffiths, and B. B. Goode, "Adaptive antenna systems," *Proceedings of the IEEE*, vol. 55, pp. 2143–2159, December 1967.

[16] J. Capon, "High-resolution frequency-wavenumber spectrum analysis," *Proceedings of the IEEE*, vol. 57, pp. 1408–1418, August 1969.

[17] R. T. Compton, *Adaptive antennas: concepts and performance*. Prentice-Hall Englewood Cliffs, NJ, 1988.

[18] S. Haykin, *Adaptive Filter Theory*. Englewood Cliffs, New Jersey: Prentice-Hall, Inc., Fourth ed., 2001.

[19] D. Moelker, E. van der Pol, and Y. Bar-Ness, "Adaptive antenna arrays for interference cancellation in GPS and GLONASS receivers," in *IEEE Position Location and Navigation Symposium*, pp. 191–198, IEEE, 1996.

[20] D. J. Moelker, "Multiple antennas for advanced GNSS multipath mitigation and multipath direction finding," in *Proceedings of the 10th International Technical Meeting of the Satellite Division of The Institute of Navigation (ION GPS)*, pp. 541–550, 1997.

[21] A. Brown and N. Gerein, "Test results of a digital beamforming GPS receiver in a jamming environment," in *Proceedings of ION GPS*, 2001.

[22] R. G. Lorenz and S. P. Boyd, "Robust beamforming in GPS arrays," in *Proceedings of the 2002 National Technical Meeting of The Institute of Navigation*, pp. 409–427, 2002.

[23] M. G. Amin and W. Sun, "A novel interference suppression scheme for global navigation satellite systems using antenna array," *IEEE Journal on Selected Areas in Communications*, vol. 23, pp. 999–1012, May 2005.

[24] D. S. D. Lorenzo, J. Gautier, J. Rife, P. Enge, and D. Akos, "Adaptive array processing for GPS interference rejection," pp. 618–627, 2005.

[25] D. S. D. Lorenzo, *Navigation accuracy and interference rejection for GPS adaptive antenna arrays*. PhD thesis, Stanford University, 2007.

[26] Y. Zheng, "Adaptive antenna array processing for GPS receivers," Master's thesis, The University of Adelaide, 2008.

[27] S. K. Kalyanaraman and M. S. Braasch, "Adaptive array phase control using an integrated software GPS signal processing architecture," in *ION GNSS 21st. International Technical Meeting of the Satellite Division*, September 2008.

[28] V. Behar, C. Kabakchiev, G. Gaydadjiev, G. Kuzmanov, and P. Ganchosov, "Parameter optimization of the adaptive MVDR QR-based beamformer for jamming and multipath supression in GPS/GLONASS receivers," in *Proceedings of the 16th Saint Petersburg International Conference on Integrated Navigation systems*, pp. 325–334, 2009.

[29] M. Trinkle and D. Gray, "GPS interference mitigation; overview and experimental results," in *Proceedings of the 5th International Symposium on Satellite Navigation Technology & Applications*, 2001.

[30] Navstar GPS Joint Program Office, *Navstar GPS Space Segment/Navigation User Interfaces (IS-GPS-200F)*, September 2011.

[31] A. Papoulis and S. U. Pillai, *Probability, Random Variables, and Stochastic Processes*. 4th ed., 2002.

[32] J. J. Spilker, *Global Positioning System: Theory and Applications, Vol 1.*, ch. ch. 3: Signal Structure and Theoretical Performance, pp. 57–119. American Institute of Aeronautics and Astronautics, 1996.

[33] H. L. V. Trees, *Optimum Array Processing*, vol. IV of *Detection, Estimation, and Modulation Theory*. New York: John Wiley and Sons, Inc., 2002.

Development and test of a digitally-steered antenna array for the Navigator GPS receiver

Heitor David Pinto
NASA Goddard Space Flight Center

November 6, 2012

Outline

- Introduction
  - Navigator GPS receiver
  - Antenna arrays and beamforming
- Development of antenna array for Navigator
  - Components
  - GPS signal simulator
  - Beamforming algorithms
- Results
  - Simulated and live-sky signals
  - Simulation of near-far interference
  - Simulation of multipath interference
- Conclusion and future work

Introduction

- Global Positioning System (GPS)
  - Satellite navigation system developed by the United States military, became fully functional in 1995
  - Signal levels and availability are adequate for users on or near Earth

- Navigator
  - GPS receiver developed at NASA for use in high orbits
  - Increase in sensitivity achieved with fast acquisition
  - Ten times more sensitive than traditional GPS receivers (25 vs. 35 dBHz)
  - Currently included in Global Precipitation Measurement (GPM) and Magnetospheric Multiscale (MMS) missions

- Next-generation Navigator goals
  - Further increase signal-to-noise ratio (SNR) by 10 dB or more (15 dBHz)
  - Reduction of interference in near-far problem and multipath signals

Traditional GPS receiver: sensitive to 35 dBHz

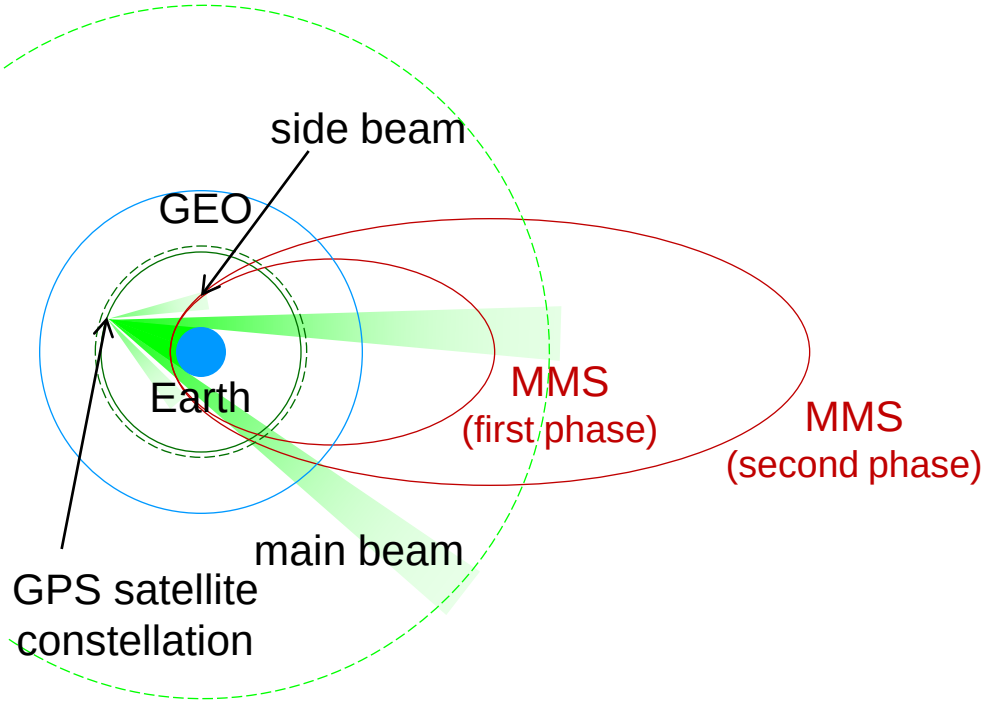

Moon

orbit of GPS satellites
geosynchronous Earth orbit
GPS side beams at 35dBHz
GPS main beams at 35dBHz

Current-stage Navigator: sensitive to 25 dBHz

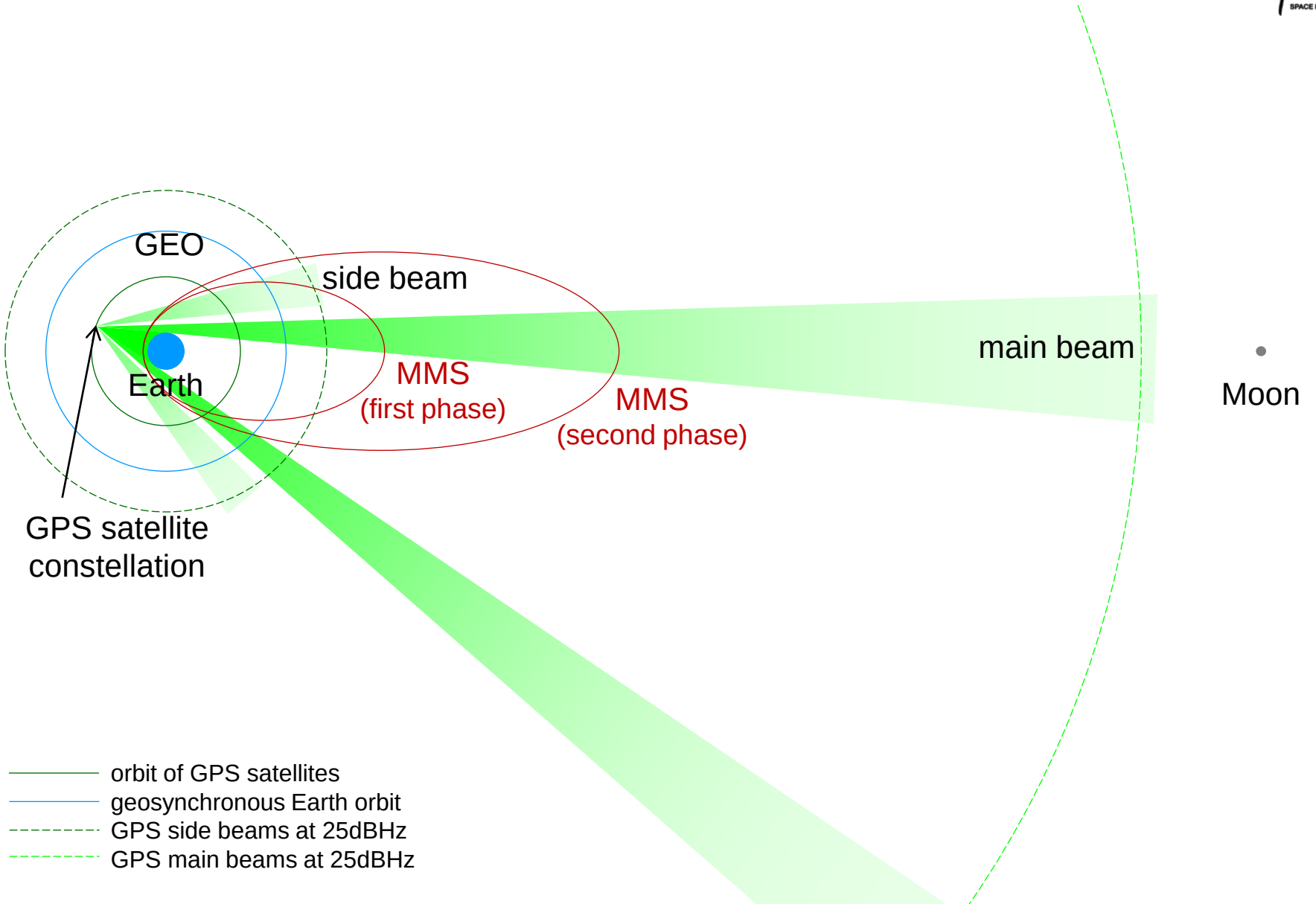

Next-generation Navigator: sensitive to 15 dBHz

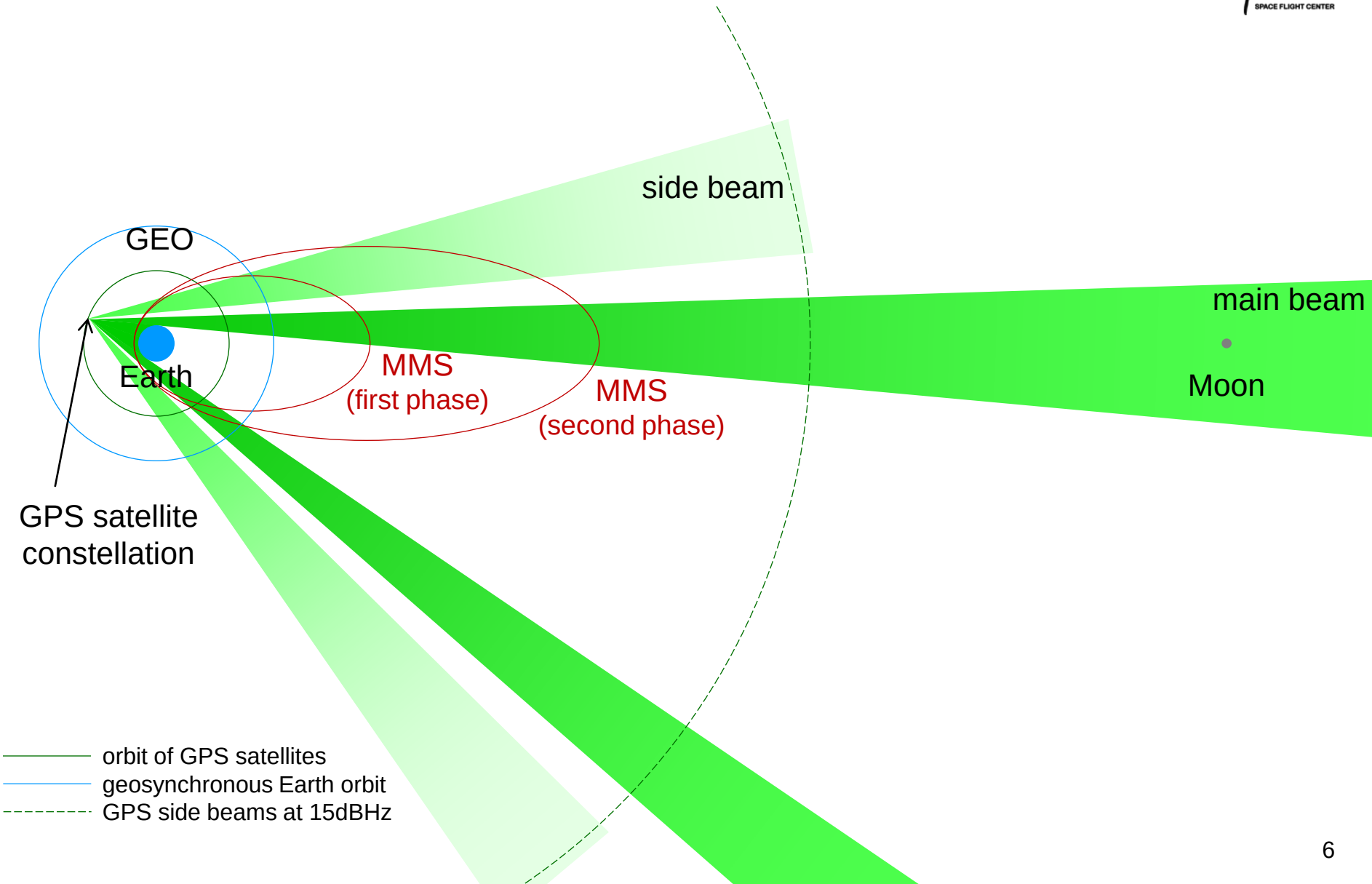

Navigator: interference environment

- Near-far problem: strong signal from a nearby transmitter prevents acquisition of weaker signals from transmitters farther away
  - Occurs when receiver is close to a GPS satellite

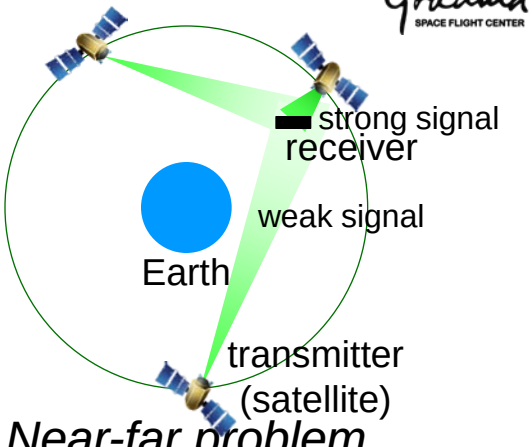

Near-far problem

- Multipath interference: combination of multiple rays degrades signal level and causes error in GPS measurements due to additional delays
  - Occurs near reflective surfaces, common on Earth and in spacecraft
  - ns, it is the dominant source of error

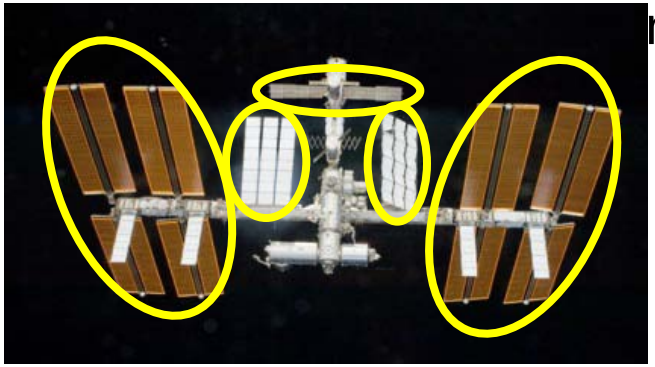

Reflective surfaces in spacecraft

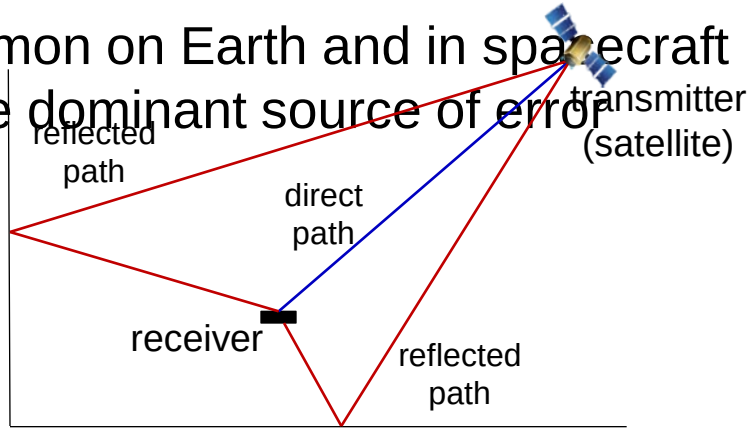

Multipath signals

Antenna arrays and beamforming

- The use of an antenna array with beamforming methods is an effective way to achieve both an increase in SNR and reduction of interference
  - Beamforming is the formation of beam patterns through the selection of coefficients or excitations to each antenna to combine the signals
  - Ideally, the main beam is steered toward the signal of interest, amplifying it, and nulls are steered toward interference, reducing them

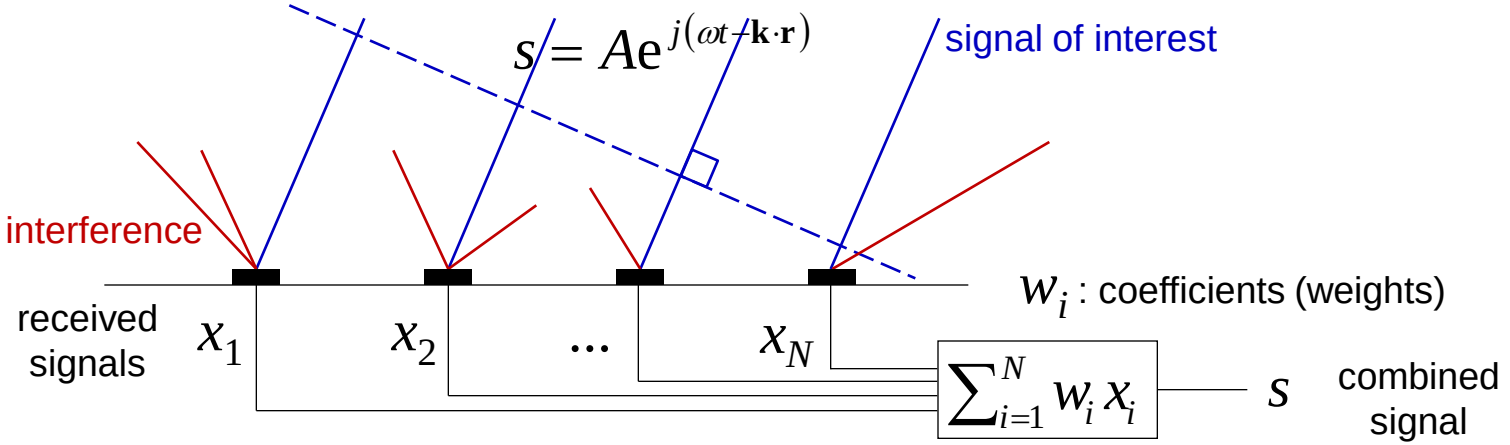

Beamforming with antenna array

Navigator with antenna array: components

Antenna array:
- signal reception
- amplification

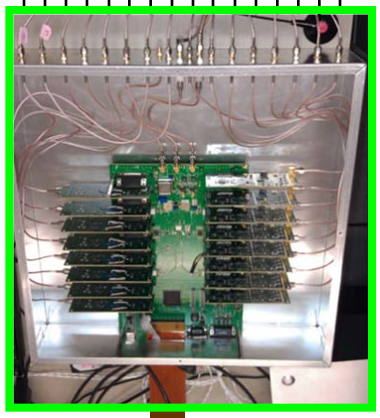

Front-end:
- frequency conversion
- filter
- sampling

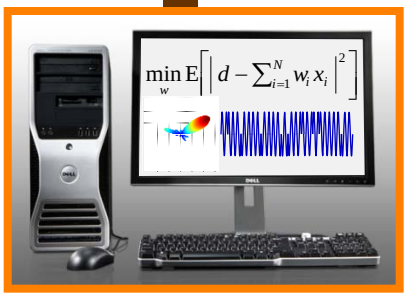

Software:
- simulations
- beamforming
- acquisition and tracking of GPS signals
- calculation of position, velocity and time (PVT)

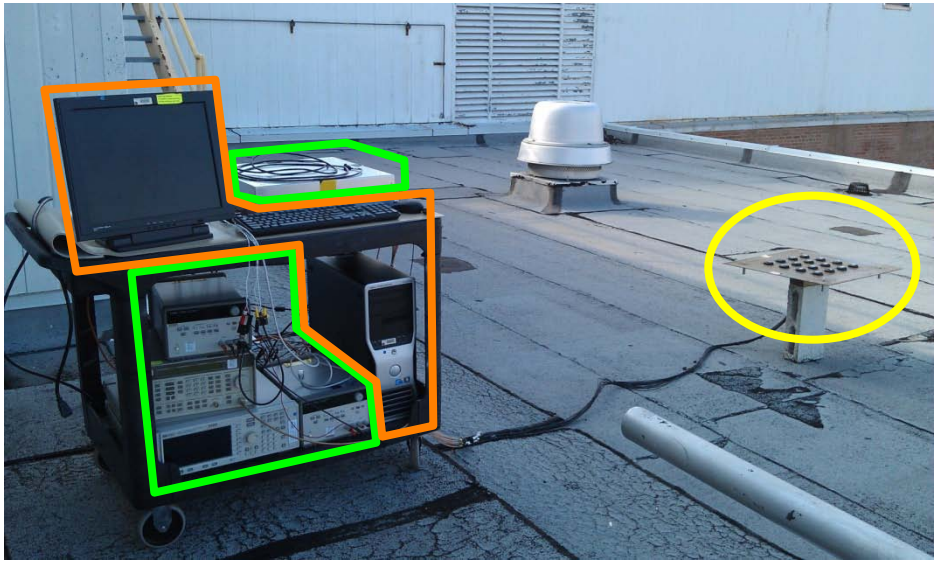

Navigator GPS receiver with antenna array

GPS signal simulator

- Simulator needed to study beamforming algorithms and test different signal levels and interference scenarios
  - Calculates dynamics of satellites and receiver, in low time steps
  - Generates GPS signals consistent with dynamics, interpolating to sampling times
  - Computes signals from each satellite as received by each antenna in an arbitrary array, approximating delays between antennas as phase shifts
  - Stores simulated signals in a file, to be read by the Navigator GPS receiver software
  - Supports near-far and multipath interference

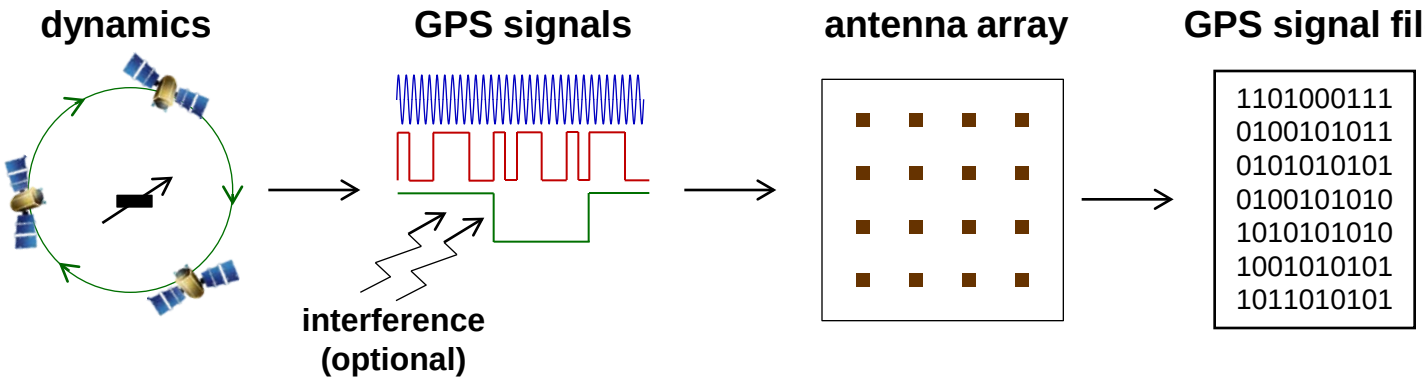

GPS signal simulator sequence

Beamforming algorithms

= best

Beamforming method	Traditional	Least mean squares (LMS)	Minimum variance distortionless response (MVDR)
Criteria	maximize gain at desired direction $w_i = \mathrm{e}^{j\mathbf{k}\cdot\mathbf{r}_i}$	minimize difference from reference signal $\min_w \mathrm{E}\left[\left\| r - \sum_{i=1}^{N} w_i x_i \right\|^2\right]$	minimize power except at desired direction $\min_w \mathrm{E}\left[\left\| \sum_{i=1}^{N} w_i x_i \right\|^2\right]$, $\sum_{i=1}^{N} w_i \mathrm{e}^{-j\mathbf{k}\cdot\mathbf{r}_i} = 1$
Calculation	direct	iterative	iterative
Computation cost	low	high	high
Requires known direction of signal of interest	yes	no	yes
Requires calibration	yes	no	yes
Reduces near-far interference	may	partially	yes
Reduces multipath interference	may	no	yes

- The best method to use depends on knowledge of directions of signals and availability of processing power

Results: simulated and live-sky signals (without interference)

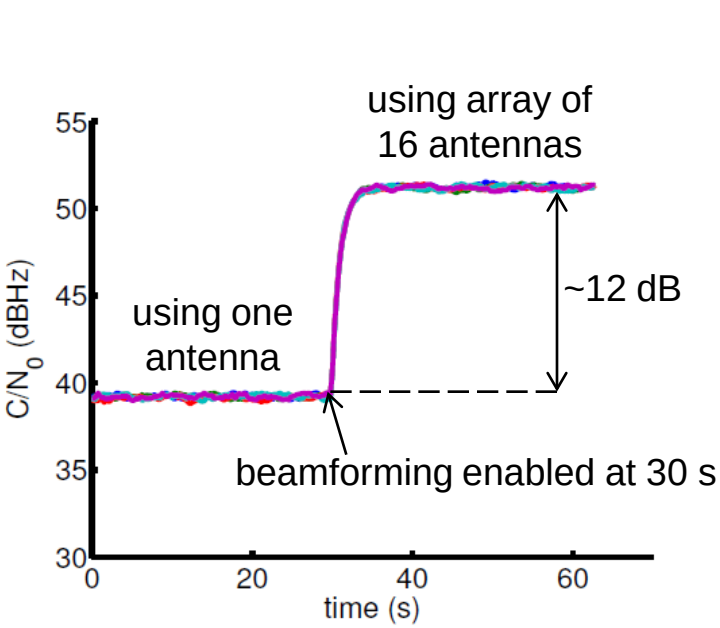

Simulated signals

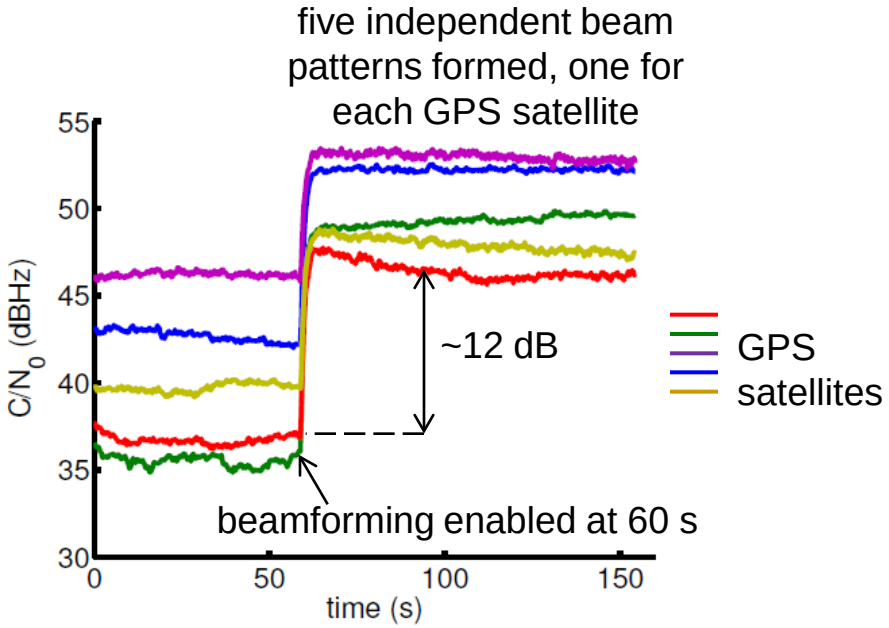

Live-sky signals

SNR before and after beamforming

Results: simulation of near-far interference

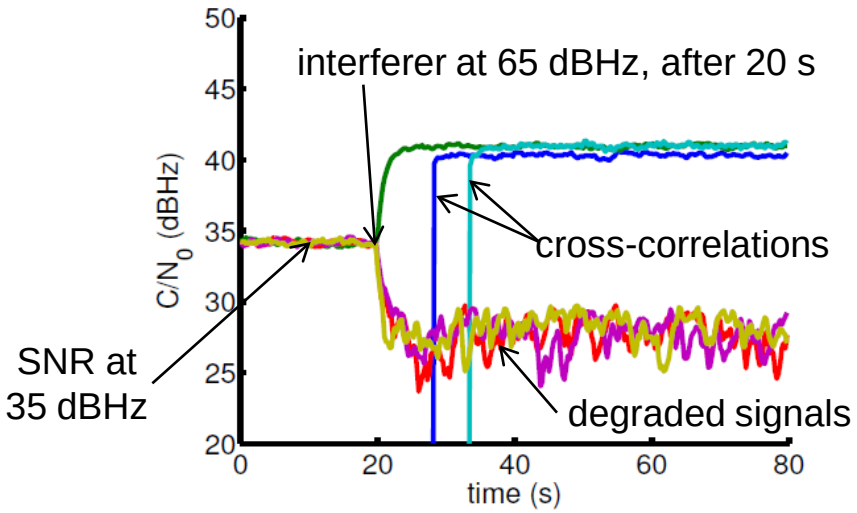

One antenna

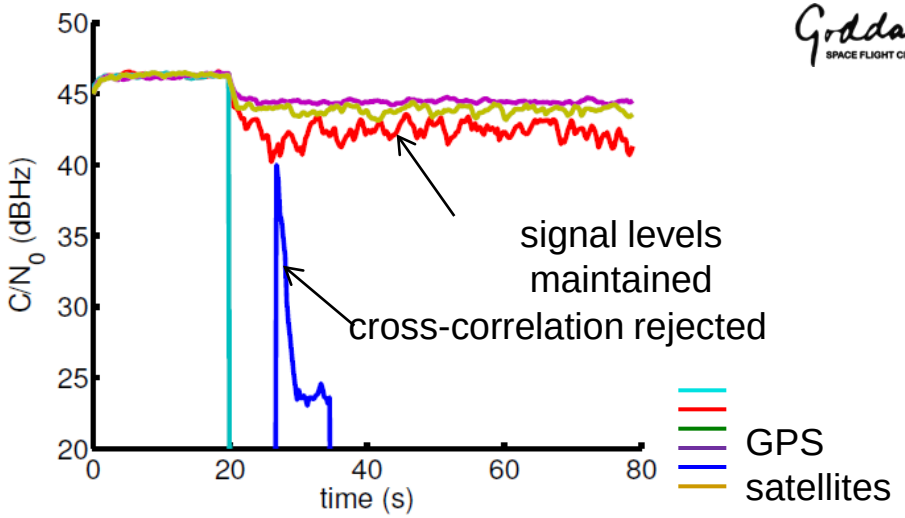

Traditional beamforming

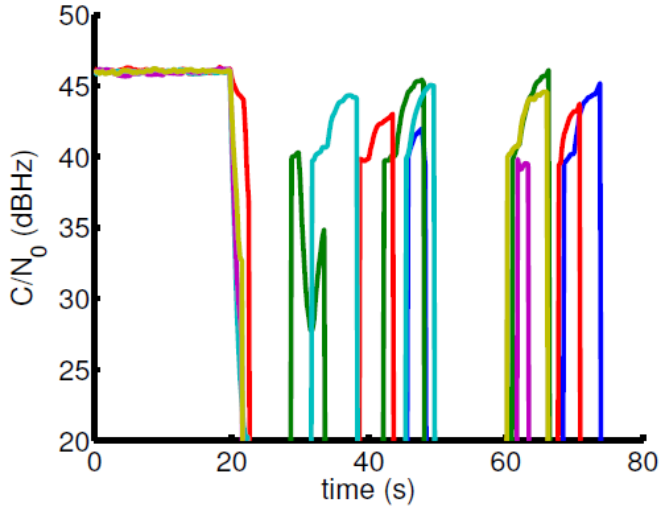

LMS

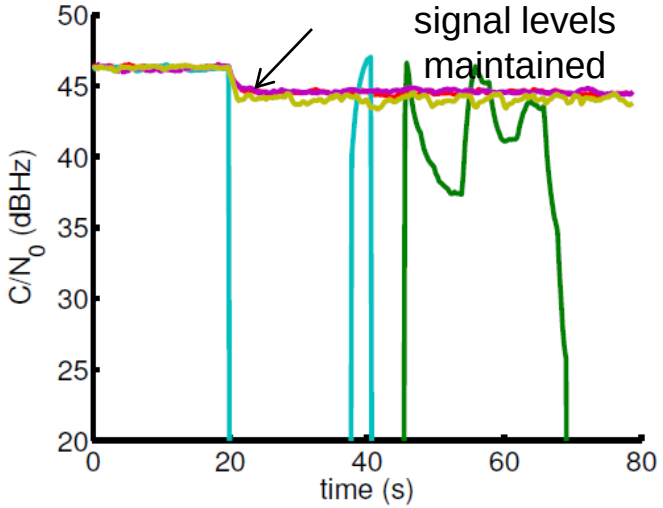

MVDR

SNR with near-far interference

Results: simulation of multipath interference

- One direct signal and three multipath signals, for one GPS satellite
- All signals have equivalent power and differ only in phase

● signal of interest
◆ interfering signal

Beam pattern, LMS

Beam pattern, MVDR

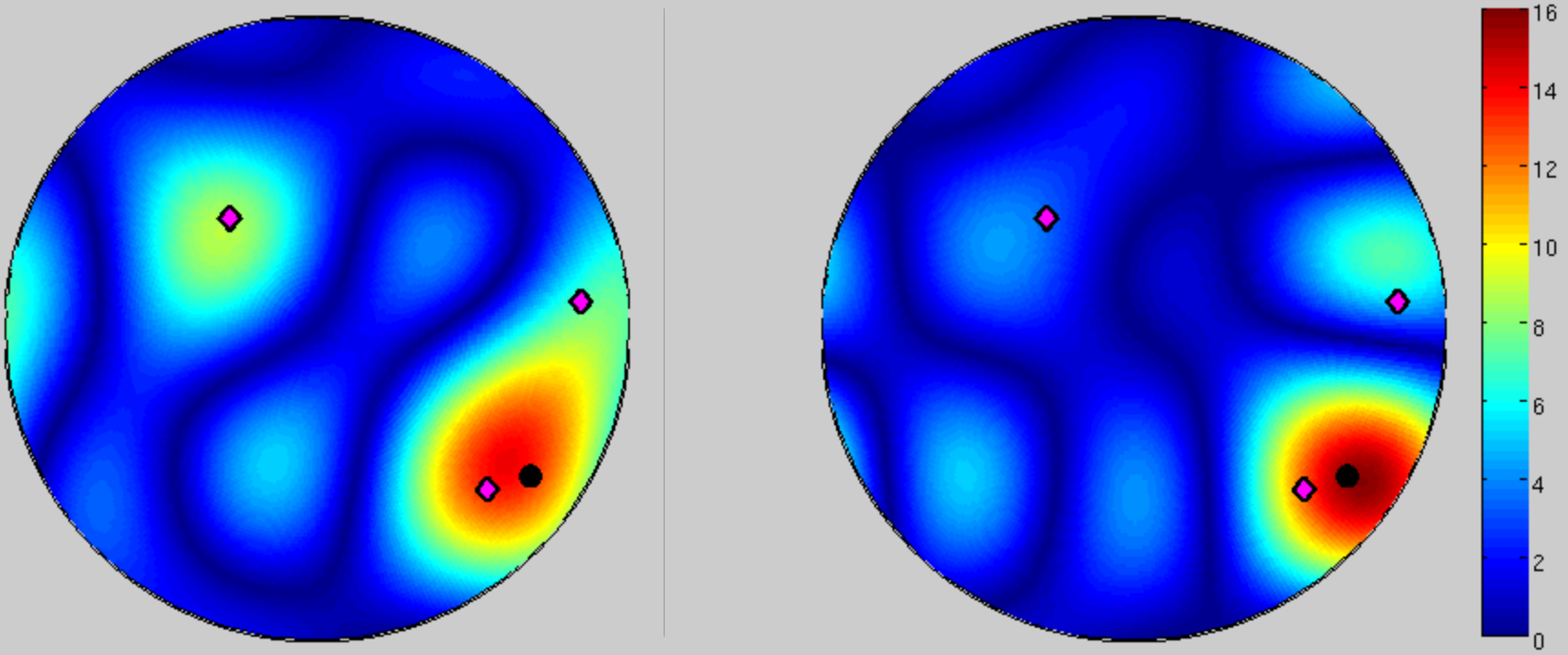

Beam pattern of antenna array under multipath interference

Results: simulation of multipath interference

- One direct signal and one multipath signal, for each of five GPS satellites
- Each multipath signal has a different delay and direction of arrival
- All signals have equivalent power (45 dBHz)

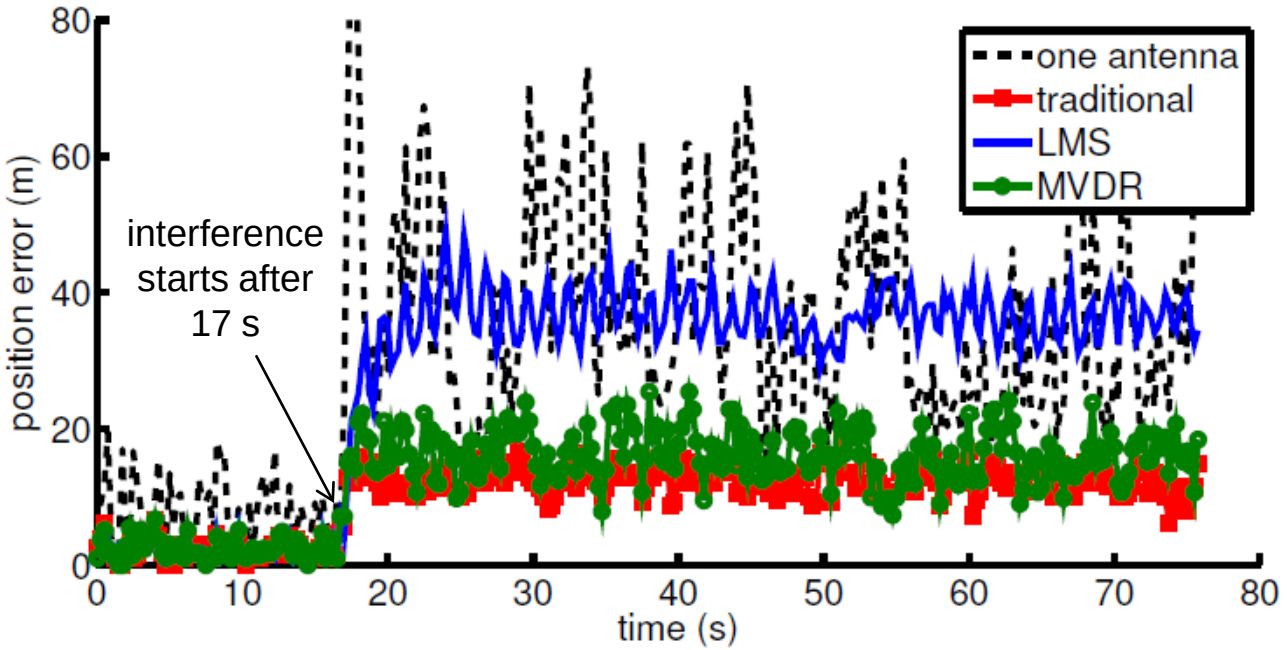

Error in position with multipath interference

Conclusion and future work

- A digitally-steered antenna array was simulated, designed and built for the Navigator GPS receiver
- Preliminary results from both simulated and live-sky signals are promising, and demonstrate the expected gains in sensitivity and mitigation of interference

- Future work: mature this technology and prepare for flight
  - More thorough analysis of interference scenarios and stability of beamforming algorithms
  - Port beamforming capability to Navigator platform in a field-programmable gate array (FPGA) and miniaturized front-end
  - Possible applications in satellite-servicing missions, such as Restore, and in experiments at the International Space Station (ISS) which require precise position or timing, such as the Neutron Star Interior Composition Explorer (NICER)

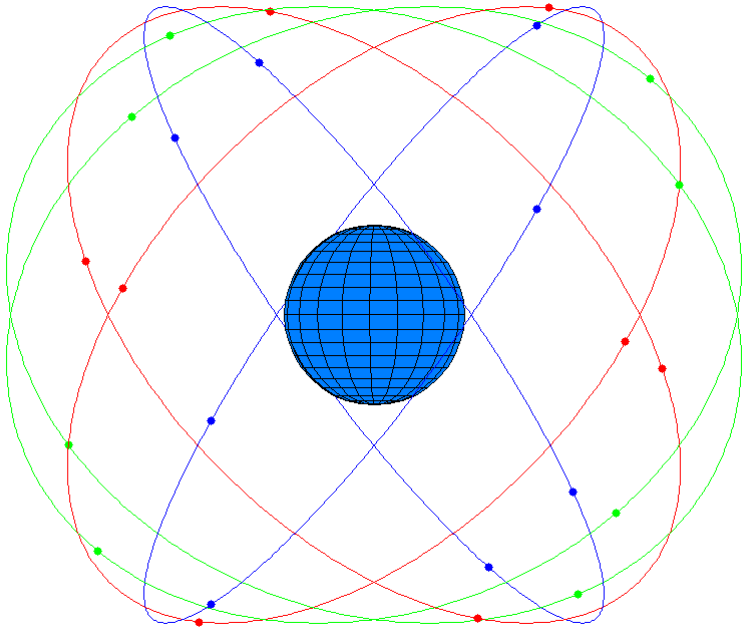

Thank you

Acknowledgments:
Jennifer Valdez, Luke Winternitz, Munther Hassouneh, Samuel Price, Lawrence Han, L. Todd Bentley, Harry Stello, Anthony Marzullo,
Cornelis du Toit, Rafael Rincón, Charles Clagett, Lamar Dougherty